Available online at www.sciencedirect.com
ScienceDirect
Journal of the European Ceramic Society 27 (2007) 1017–1021
www.elsevier.com/locate/jeurceramsoc

Optimization of chromium oxide nanopowders dispersion for spray-drying

Audrey Cellard [a,*], Rachid Zenati [a], Vincent Garnier [a], Gilbert Fantozzi [a], Guy Baret [b]

[a] *INSA Lyon, GEMPPM UMR CNRS 5510, Villeurbanne 69621, France*
[b] *DGTec, 178 Rue Mayoussard, Moirans 38430, France*

Available online 5 June 2006

Abstract

The aim of this work is to produce spherical micron-sized granules by spray-drying. This technique requires stable and well-dispersed suspensions. The targeted application for such granules is the development of wear resistant Cr_2O_3 nanostructured coatings by plasma projection. The work reported in this paper was performed to develop and to optimize Cr_2O_3 nanopowders dispersion by a ball milling method for producing granules.

Physical, structural and microstructural properties of Cr_2O_3 nanopowders were followed by XRD analysis, helium pycnometer density, gas adsorption (BET), SEM and TEM observations.

The choice of suitable dispersant was determined by zeta potential measurements. The dispersant amount has been optimized from the rheological behavior of slurries containing 30 wt.% nanopowders. Slip stabilization was investigated by sedimentation tests and zeta potential measurements. The influences of milling time, milling balls diameter and milling balls to powder ratio were studied by granulometric measurements. A well-dispersed and stable aqueous Cr_2O_3 slip, suitable for spray-drying, was achieved.

Keywords: Milling; Suspensions; Wear resistance; Cr_2O_3; Nanopowders

1. Introduction

The aim of this research is the development of wear resistant plasma sprayed nanostructured coatings from nanopowders. Indeed, these coatings have been recognized to exhibit remarkable and technologically attractive properties, such as a better wear resistance.[1] These nanostructured coatings have applications in various fields such as automotive or aerospace.[2] One of the main problems to prepare nanocoatings by plasma projection is to feed nanopowders into the plasma jet.[3] Indeed, nanopowders, strongly agglomerated, have a very poor flowability, a low mass and usually adhere to the walls of the feeding system.[4] To overcome this problem, nanoparticles can be spray-dried from a slip to obtain micrometer-sized granules with good flowability. The elaboration of a well-dispersed and stable suspension is an essential step for spray-drying.[5]

The slip stability is determined by the nature of the interactions between particles during collisions due to Brownian motion. From the DLVO theory, developed by Derjaguin, Landau, Verwey and Overbeek,[6] interactions between colloidal particles are a superposition of electrostatic repulsion and Van der Waals attraction. Therefore, a colloidal dispersion can be obtained if the repulsive forces are strong enough to counteract the Van der Waals attraction forces. The repulsion between particles arises from two different sources, one is due to the electrical double layers located around the particles, and the other is due to the adsorbed layers composed of non-ionic materials, including adsorbed molecules of the dispersion medium. These two repulsive mechanisms, which are crucial to stabilize colloidal dispersions, are termed electrical stabilization and sterical stabilization, respectively.[6] A combination of these two effects can be used to obtain a stable suspension. Slight modifications of the particles environment, like the pH, may disturb the suspension stability.

The present paper deals with the nanopowders dispersion process. The aim of this study is to obtain a well-dispersed and stable suspension of chromium oxide Cr_2O_3 nanopowders, suitable for spray-drying, by a ball milling technique. Chromium oxide has an excellent wear resistance and a high hardness.[7] The effect of the nature of dispersant, dispersant amount, desagglomeration time, milling balls diameter and milling balls ratio has been investigated. The well-dispersed and stable suspension achieved has been spray-dried and Cr_2O_3 granules with an homogeneous distribution centered on 50 μm have been produced.

* Corresponding author. Tel.: +33 4 72 43 62 39; fax: +33 4 72 43 85 28.
E-mail address: Audrey.Cellard@insa-lyon.fr (A. Cellard).

0955-2219/$ – see front matter © 2006 Elsevier Ltd. All rights reserved.
doi:10.1016/j.jeurceramsoc.2006.04.132

2. Experimental procedures

Cr_2O_3 nanopowders, obtained by a sol–gel method (DGTec, France), were used in this study. The mean particle diameter was 100 nm. To analyse the nanopowders crystallographic structure, a standard powder diffractometer (Rigaku) with Cu Kα radiation and a graphite monochromator was used. The powders density was obtained using an helium pycnometer (Micromeritics, AccuPyc 1330). Powders morphology was examined by Scanning Electron Microscopy (SEM) with a JEOL 840 ALGS and by Transmission Electron Microscopy (TEM) with a JEOL 2010 FEG. The specific surface area was measured by Brunauer, Emmett and Teller (BET) method (Micromeritics, ASAP 2010).

Nanopowders were dispersed in deionized water with deflocculant in horizontal rolling mill for several hours with alumina milling media.

The rheological behavior of the slips was characterized at 25 °C by a rotary viscosimeter HAAKE VT 501. Zeta potential measurements versus pH were realized by Zetasizer 3000 HSA (Malvern Instruments) in diluted suspension and by Acousto-Sizer II (Colloidal Dynamics Inc.) in concentrated suspension. Particles size distribution was measured using a laser diffractometer (Malvern Instruments, Mastersizer HYDRO 2000).

Ten dispersants were tested. For the adequate dispersant, the optimal amount has been determined and the pH adjusted. The influence of milling time has been investigated. Two different alumina milling balls diameters have been studied: 2.4 mm diameter and 0.9–1.9 mm diameter. Eight different weight ratios, defined as milling balls quantity on powder content, have been tested with 0.9–1.9 mm milling balls diameter: 3, 5, 6, 7, 8, 9,10 and 15.

3. Results and discussion

3.1. Characterization of Cr_2O_3 nanopowders

Cr_2O_3 nanopowders observed by XRD show pure hexagonal eskolaite phase and a perfect superposition is obtained with the JCPDS 85-0869 card (cf. Fig. 1). Cr_2O_3 crystallizes in the rhombohedral crystal system.

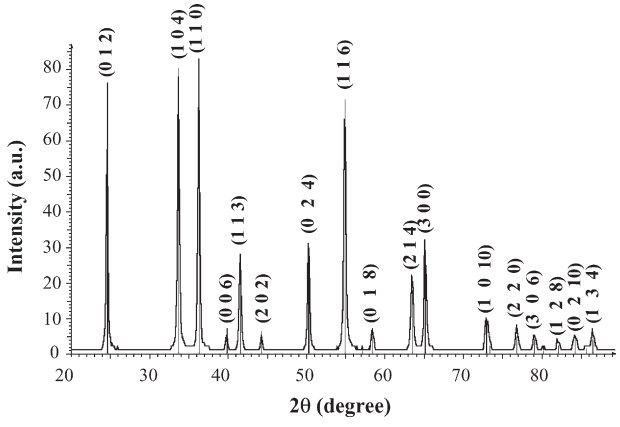

Fig. 1. Diffraction diagrams of Cr_2O_3 nanopowders and of the JCPDS 85-0869 card.

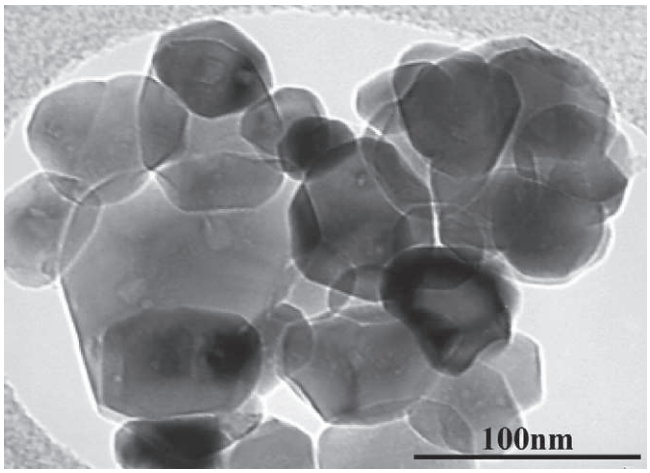

Fig. 2. Cr_2O_3 individual nanoparticles (TEM observations).

However, TEM observations of Cr_2O_3 nanopowders confirm the nanostructured features of the starting powder (cf. Fig. 2). The Cr_2O_3 nanopowders specific surface area, measured by BET, is 16 $m^2\,g^{-1}$.

Nanopowders have a measured density of $5.10 \pm 0.02\ g\,cm^{-3}$ and theoretical density indicated on the JCPDS 85–0869 card is $5.235\ g\,cm^{-3}$. The difference between these values is due to the nanopowders crystallinity. Indeed, starting nanopowders have been previously treated by DGTec at 900 °C for 1 h and for comparison, thermal treatments at 1000, 1100 and 1200 °C for 1 h have also been performed. Fig. 3 shows that the nanopowders density increases with temperature and stabilizes at the theoretical density value. This means that the crystallization of the starting nanopowders was not complete and that amorphous phase located around particles was responsible of the low density.

3.2. Cr_2O_3 nanopowders dispersion

3.2.1. Dispersant choice

To select the most appropriate dispersant, zeta potential measurements in aqueous diluted suspension have been carried out with several dispersants (cf. Fig. 4). The best dispersant for considered nanopowders corresponds to the dispersant with the highest zeta potential value. In fact, a higher zeta potential value leads to higher repulsive forces between particles and conse-

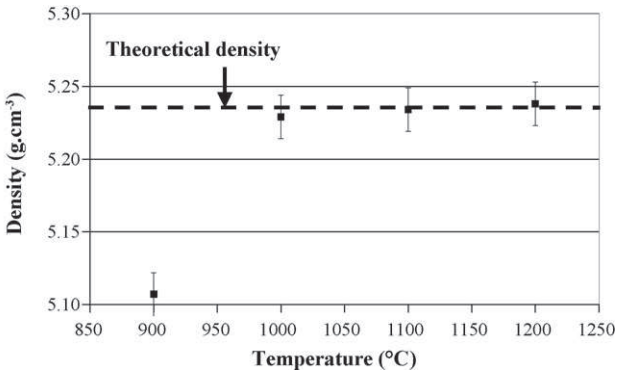

Fig. 3. Evolution of the Cr_2O_3 nanopowders density with temperature.

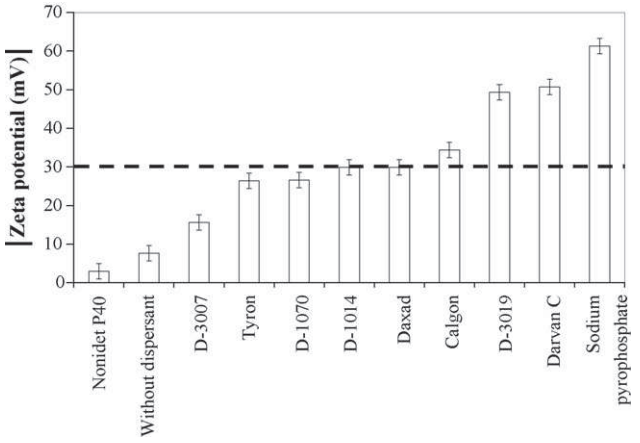

Fig. 4. Zeta potential of Cr_2O_3 suspensions depending on the dispersant choice.

quently higher suspension stability. As suspensions with a zeta potential higher than |30 mV| are considered stable,[8] all dispersants leading to a zeta potential below this value cannot be used. From Fig. 4, three products are then potential dispersants for chromium oxide nanopowders dispersed in these conditions: sodium pyrophosphate, DarvanC (ammonium salt, R.T. Vanderbilt Company, Inc., USA) and D-3019 (ammonium salt, Rohm and Haas Company). Although sodium pyrophosphate leads to the highest zeta potential, the presence of sodium is unsuitable for the dispersion of pure Cr_2O_3 because of contamination. The second best dispersant is DarvanC. Therefore, DarvanC was selected to disperse Cr_2O_3 nanopowders. DarvanC bears carboxylic groups with negative charges which adsorb on particles surface and create simultaneously a sterical stabilization and an electrical stabilization.

3.2.2. Dispersant amount optimization

Slips with solid content of 30 wt.% Cr_2O_3 nanopowders were prepared. The dispersion state is directly correlated to the rheological behavior of the slurry. The minimum of viscosity corresponds to the maximum of mobility and to an optimal dispersion.[6] To determine the optimum dispersant amount, the slurry viscosity was then measured at fixed shear rate (109 s^{-1}) and natural pH of the slip (pH 6 ± 0.1) with different DarvanC amount after 24 h of milling. Alumina balls have been used, with a diameter of 2.4 mm and a weight ratio of 3. It is shown on Fig. 5 that the curve presents a minimum between 0.9 and 1.5 wt.% of DarvanC amount. This minimum corresponds to the optimum of dispersion.

The influence of solid content on optimal dispersant amount has been investigated. The Fig. 6 represents the viscosity versus dispersant amount at a shear rate of 109 s^{-1} for two different solid content: 30 and 40 wt.%. It shows that the powder content in the slurry has no influence on the optimal dispersant amount, which is still equal to about 1.3 wt.% when powder content increase from 30 to 40 wt.%. However, minimum viscosity area is wider for 30 wt.% than for 40 wt.% and the increase of the powder content leads to the increase of the slip viscosity, which is coherent since the distance between particles becomes shorter.

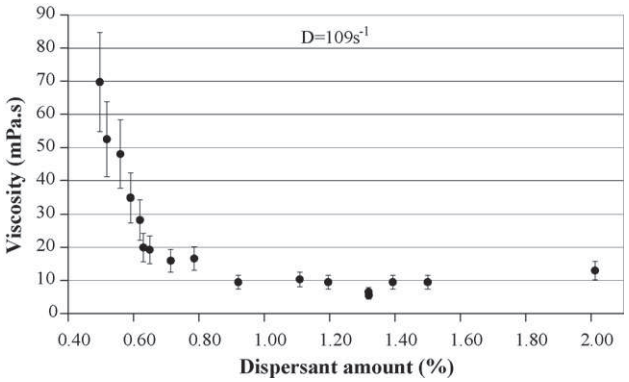

Fig. 5. Evolution of the slip viscosity with the dispersant amount.

3.2.3. Study of working pH by zeta potential measurements in concentrated suspension and by sedimentation measurements

pH adjustment has been studied by zeta potential measurements in concentrated suspension. The dispersion stability is directly dependent to pH which is a determinant parameter related to the electrostatic charges on the surface of oxide particles.[8] Measurements have begun at natural pH of the slip (i.e. pH 6). Then, slip pH has been increased towards basic pH by addition of ammoniac 1 M and after that, towards acid pH by addition of hydrochloric acid 1 M.

The evolution of zeta potential values versus pH shows that the highest zeta potential values ($\xi > 50$ mV) are obtained in the range of the pH 6–10 (cf. Fig. 7). However the natural pH of these slips is about 6. Consequently, the repulsive forces between individual Cr_2O_3 nanoparticles are thus maximized to keep each particle separated from each other and to prevent them from flocculation, either in diluted suspension (cf. Fig. 4) or in concentrated suspension (cf. Fig. 7). The isoelectric point is around pH 3. At this pH, there are no repulsive forces. The suspension is then unstable and floculates.

Slips stability was evaluated by the sedimentation test. The test was conducted in three 10 mL graduated cylinder tubes by observing the height of the interface between the setting suspension and its supernatant during 12 days.

The sedimentation of a single particle, calculated by Stockes' law, is higher than that obtained with the well-dispersed suspension. Thus, the stability of the slips is well confirmed.

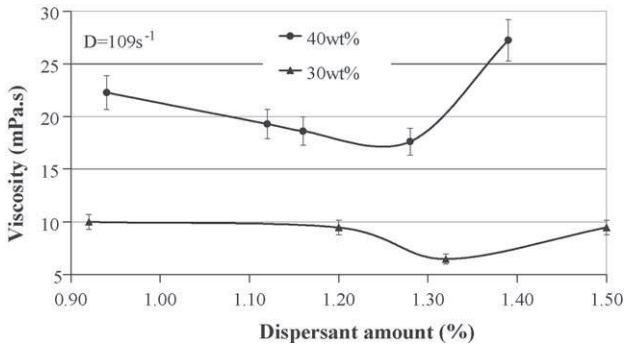

Fig. 6. Influence of the powder content on the optimal dispersant amount.

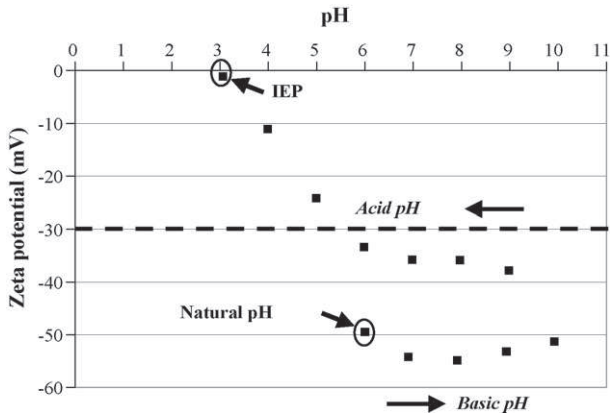

Fig. 7. Zeta potential values vs. pH.

3.2.4. Influence of desagglomeration time on particles size distribution

The influence of the milling time with alumina balls diameter 2.4 mm and a weight ratio of 3 has been studied by granulometric measurements. As shown on Fig. 8, after 24 h of milling, the peak representing the agglomerates is centered on 3 μm. After 43 h, this peak moves towards smaller particles size and becomes centered on 900 nm which means that more agglomerates are broken after 43 h than 24 h. This observation is confirmed by mean diameter values. After 24 h, mean diameter is equal to 1.3 μm whereas after 43 h, it decreases until 163 nm. These measurements show consequently an important influence of desagglomeration time on granulometric distribution with a shift in the distribution towards a smaller particles size region when the milling time is increased.

3.2.5. Influence of milling balls diameter on particles size distribution

Two different alumina milling ball types have been studied on particles size distribution by granulometric measurements after 24 h with a weight ratio of 3: milling balls with a single diameter of 2.4 mm and milling balls whose diameters follow a Gauss distribution (diameters between 0.9 and 1.9 mm). From Fig. 9, milling balls diameter 0.9–1.9 mm are more efficient to reduce the particles size than milling balls diameter 2.4 mm. Indeed, with milling balls diameter 2.4 mm, agglomerates peak is centered on 3 μm with a mean diameter value equal to 1.3 μm,

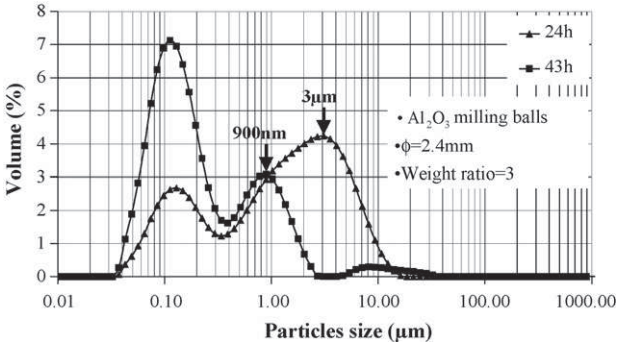

Fig. 8. Influence of desagglomeration time on particles size distribution.

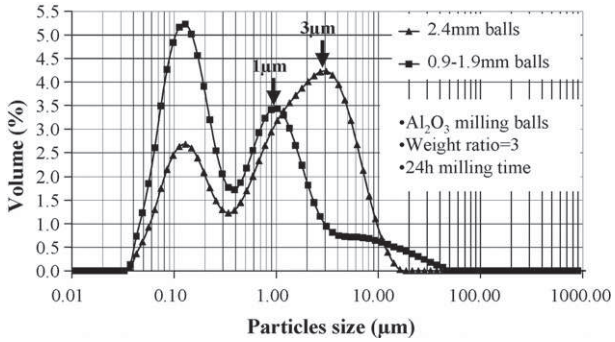

Fig. 9. Influence of milling balls diameter on particles size distribution.

as previously, while with milling balls diameter 0.9–1.9 mm, agglomerates peak is centered on 1 μm with a mean diameter value of 299 nm. As a result, alumina milling balls with a diameter of 0.9–1.9 mm have been used afterwards.

3.2.6. Optimization of 0.9–1.9 mm diameter milling balls weight ratio and milling time

The influence of 0.9–1.9 mm diameter milling balls weight ratio was investigated on particles size distribution by granulometric measurements. Eight different weight ratios have been tested: 3, 5, 6, 7, 8, 9, 10 and 15. Moreover, it has been shown (cf. Section 3.2.4) that desagglomeration time has a significant influence on granulometric distributions. As a result, for each weight ratio tested, desagglomeration time has been studied simultaneously and milling times indicated on Fig. 10 correspond to the optimum desagglomeration times. Fig. 10 shows granulometric curves obtained for the weight ratios 3, 7 and 15. For a weight ratio of 3 after 70 h, mean diameter obtained is 130 nm. From this curve, we can see that important agglomerates, superior to 10 μm, are not destroyed. For a weight ratio of 15 after 26 h, observations are similar. With a weight ratio of 7 after 95 h, no agglomerates peak is present. The nanometric peak achieved in these conditions is the highest and mean diameter value is the weakest: 100 nm. The best dispersion is then achieved with the 0.9–1.9 mm diameter alumina balls after 95 h of milling with an optimum weight ratio of 7. In these conditions, the mean diameter obtained is comparable with the supplier specifications.

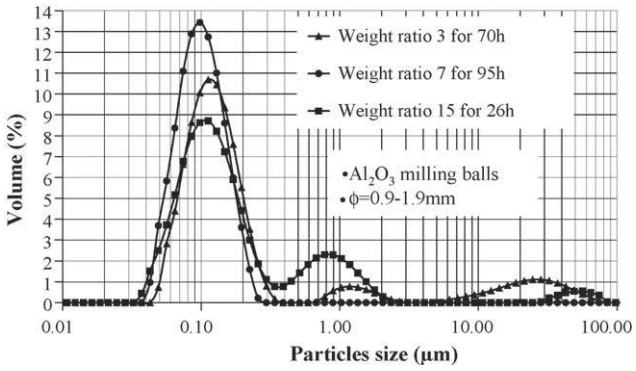

Fig. 10. Influence of milling balls weight ratio on particles size distribution after optimal milling time.

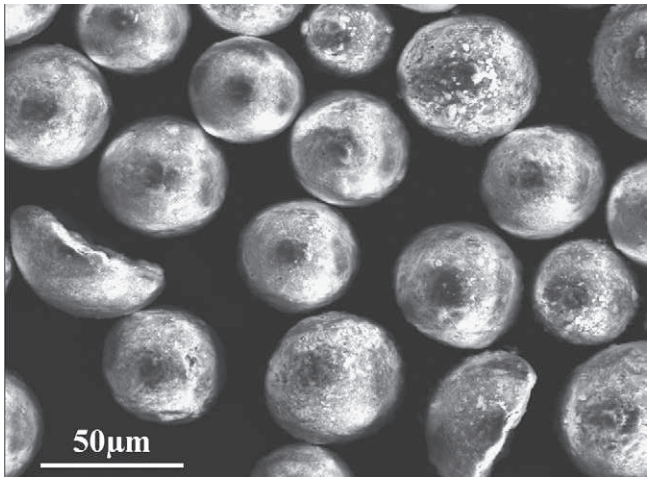

Fig. 11. Cr_2O_3 granules obtained from optimized slip by spray-drying.

All these process parameters optimizations have allowed to obtain a well-dispersed and stable Cr_2O_3 aqueous slip which has been spray-dried. Full chromium oxide Cr_2O_3 granules have then been achieved (cf. Fig. 11). Granules size distribution is homogeneous and centered on 50 μm. Owing to their micrometer size and their spherical shape, granules flowability is high. These granules are therefore suitable for plasma projection.

4. Conclusions

Nanopowders are dispersed with DarvanC in deionized water and ball-milled in a polyethylene jar with alumina milling balls. Result analysis of the dispersion study shows that a well-dispersed and stable suspension, suitable for spray-drying, is achieved at natural pH, with 1.3 wt.% of DarvanC, after 95 h of desagglomeration with milling balls diameter 0.9–1.9 mm and a weight ratio of 7.

This optimized slip has been spray-dried. Full Cr_2O_3 granules, with an homogeneous distribution centered around 50 μm, have been achieved. The results of this spray-drying study will soon be published. Cr_2O_3 granules have been plasma-sprayed in order to obtain nanostructured coatings.

Acknowledgement

The authors thank M.C. Bartholin (Ecole des Mines de Saint-Etienne, France) for zeta potential measurements in concentrated suspension.

References

1. Liu, X., Zhang, B. and Deng, Z., Grinding of nanostructured ceramic coatings: surface observations and material removal mechanisms. *Int. J. Mach. Tools Manuf.*, 2002, **42**, 1665–1676.
2. Richard, C. S., Lu, J., Beranger, G. and Decomps, F., Study of Cr_2O_3 coatings. Part I. Microstructures and modulus. *J. Thermal Spray Technol.*, 1995, **4**, 342–346.
3. Zeng, Y., Lee, S. W. and Ding, C. X., Plasma spray coatings in different nanosize alumina. *Mater. Lett.*, 2002, **57**, 495–501.
4. Wang, Y., Jiang, S., Wang, M., Wang, S., Xiao, T. D. and Strutt, P. R., Abrasive wear characteristics of plasma sprayed nanostructured alumina/titania coatings. *Wear*, 2000, **237**, 176–185.
5. Cao, X. Q., Vassen, R., Schwartz, S., Jungen, W., Tietz, F. and Stoever, D., Spray-drying of ceramics for plasma-spray coating. *J. Eur. Ceram. Soc.*, 2000, **20**, 2433–2439.
6. Sato, T. and Ruch, R., *Stabilization of colloïdal dispersions by polymer adsorption*, *Vol 9*. Surfactant Science Series, New York, 1980, ISBN 0-8247-6970-8, 155 pp.
7. Mann, B. S. and Prakash, B., High temperature friction and wear characteristics of various coating materials for steam valve spindle application. *Wear*, 2000, **240**, 223–230.
8. Vallar, S., Houivet, D., El Fallah, J., Kervadec, D. and Haussonne, J. M., Oxide slurries stability and powders dispersion: optimization with zeta potential and rheological measurements. *J. Eur. Ceram. Soc.*, 1999, **19**, 1017–1021.